Characteristics of Cast Aluminum Alloys for Structural Components

*Stuart Wiesner¹, Kunal Wandrekar¹

1. Bukheinstrasse 2, Rheinfelden, 79618, Germany

*Corresponding address: e-mail: swiesner@rheinfelden-alloys.eu

Abstract The demand for large structural aluminum components in automotive and industrial applications drives the need for innovative high-pressure die casting (HP-DC) alloys. This study gives an overview about the exploration of advanced aluminum alloys tailored for structural use, emphasizing sustainability by incorporating high recycling content and reducing carbon footprints. Tested on machines ranging from 400 to 4400 tons, the alloys studied include AlSi10MnMg (Silafont-36), AlSi7MnMg (Silafont-33), AlSi9MnMoZr (Castasil-37), AlMg4Fe2 (Castaduct-42), AlMg4Fe1Mn1Si (Castaduct-51), and AlMg6Si2Mn (Magsimal-plus). Key findings cover mechanical properties, heat treatment, castability, riveting and welding performance, and corrosion resistance. AlSi alloys are versatile but often require heat treatment for optimal performance, while Castaduct-42 and Magsimal-plus offer excellent properties in the as cast state. Castaduct-51 allows for extensive recycling by using materials like beverage cans, whereas Magsimal-plus achieves high strength with limited recycled content. These developments support larger, thinner, high-integrity castings, aligning technological advancement with environmental goals in die casting.

Keywords: Aluminum cast alloys, high pressure die casting, structural components, recycling, sustainability, carbon footprint.

1 Introduction

1.1 Roadmap and upcycling

Sustainability in the automotive and manufacturing sectors is more crucial than ever. Reducing carbon emissions and conserving resources have driven the need for innovative aluminum alloys for high pressure die cast (HP-DC) structural components. Aluminum's lightweight, high strength, and recyclability make it ideal for lowering the environmental footprint of automotive structures.

To achieve sustainability goals, industries are shifting from primary aluminum, which involves energy-intensive production, to secondary aluminum derived from recycled materials. The trend toward larger structural components demands alloys with low carbon footprints, high recycled content, and high strength, while avoiding two-step T6 heat treatments to minimize distortion.

This paper explores next-generation aluminum alloys for HP-DC, focusing on integrating recycled content and optimizing compositions with scrap sources like wheels, cans, and extrusions. By refining heat treatments and quenching techniques, these alloys meet stringent standards for strength, durability, and corrosion resistance. This study offers insights for die casters and engineers aiming to balance performance with sustainability.



Fig. 1: Roadmap to net zero of Rheinfelden

Figure 1 shows the milestones of Rheinfelden towards a net zero carbon footprint. End of 2023, Rheinfelden became a member of the Aluminum Stewardship Initiative (IAI) [1]. Now Rheinfelden is aiming for certification of a carbon footprint calculation tool (ISO 14067) [2]. The goal is for production in Rheinfelden to be carbon neutral by 2030 (Scope 1 and 2), by 2050 including the entire supply chain (Scope 3).

Upcycling plays a key role in advancing recycling efforts ^[3, 4]. At Rheinfelden, an important project focuses on developing high-strength alloys for high-pressure die casting using low-quality scrap. This initiative boosts sustainability by reducing waste, as low-quality scrap is transformed into valuable products that would otherwise end up in landfills.

It conserves resources by decreasing the need for virgin aluminum, thereby saving natural resources and lowering energy consumption. Additionally, producing alloys from low-quality scrap consumes less energy than using virgin aluminum, reducing the overall carbon footprint. This approach also lowers production costs, enhancing manufacturers' competitiveness.

Developing high-strength alloys from low-quality scrap presents another promising path for a more sustainable aluminum industry. To maximize its benefits, careful evaluation of environmental impacts and trade-offs is essential.

1.2 Carbon footprint calculation

Many projects worldwide focuses on conserving resources and reducing the carbon footprint. The International Aluminum Institute (IAI) [5] recognizes many of these initiatives, which can be found on aluminum manufacturers' websites [6-13]. Implementing measures throughout the production chain and using secondary materials is crucial. Transparency in carbon footprint calculations is necessary, though universally accepted standards are still lacking. While the IAI and the Aluminum Stewardship Initiative (ASI, [1]) provide general frameworks, they do not specify detailed methods for calculating the carbon footprint of individual productions.

At Rheinfelden, the carbon footprint of aluminum cast alloys is calculated as part of the ISO 14067 certification process [2]. Scope 1 covers emissions from natural gas and process gas consumption, Scope 2 addresses emissions from electricity use, and Scope 3 includes emissions from the entire supply chain.

Rheinfelden selects primary aluminum suppliers carefully with a focus on traceability and certification. The carbon footprint for Scope 3 is determined by the entire process chain, from mining through refining to electrolysis. Electrolysis is the most energy-intensive step, making the use of hydropower for electricity a key measure for reducing the carbon footprint. The second most important factor is refining, which should be carried out as efficiently as possible. Thirdly, the electrodes used in electrolysis should be considered. Currently, carbon electrodes are standard, which directly emit CO₂. However, the use of ceramic, inert electrodes, which do not produce CO₂, is in the project phase.

The transport of materials has a minor impact, but is calculated as well. Primary aluminum is send via the seaport of Rotterdam (a hub for LME materials) and then by the Rhine River to Rheinfelden.

For secondary aluminum, carbon footprint estimates

consider processing (downsizing, packing) and transportation. In 2024, the carbon footprint for producing an alloy from 100% secondary material was projected to be 0.5–0.75 tons of CO_{2-eq.} per ton of alloy, aligning with data from other manufacturers. Conservative transport estimates suggest even lower values for domestic transport within Germany.

Rheinfelden aims to increase secondary content in all casting alloys, as described in the alloy chapter.

The carbon footprint of alloying elements like silicon, magnesium, manganese, zinc, and iron depends on their extraction, processing, and transport. The CO_{2-eq.} values for the individual alloying elements are based on official data provided by German authorities ^[14, 15]. By carefully selecting and optimizing these elements, the overall footprint of the alloy can be minimized. Detailed tracking of each element enables precise calculations and supports sustainable alloy development.

In 2024, Rheinfelden's average production carbon footprint was 0.3 tons of CO_{2-eq.} per ton of alloy. This includes emissions from gas for melting, oxygen burners, process gases (e.g. chlorine), and energy for preheating. Metal burnup added 0.15 tons of CO_{2-eq.} per ton of alloy. Due to Rheinfelden's wide range of alloys and batches, these values are slightly higher than those of large-scale producers but significantly lower than many foundries focused on casting optimization rather than melting efficiency.

1.3 Chatbot interface

Efficient access to information is essential in material science. One of Rheinfelden's project aims to develop a chatbot interface for instant data on aluminum cast alloys, integrating information from technical reports, publications, Leporello catalogue and the carbon footprint calculation tool. The chatbot helps engineers, designers and manufacturers to improve decision-making and efficiency.

The first step involved digitizing Rheinfelden's alloy data, including compositions, properties, and environmental impacts. Advanced natural language processing (NLP) ensures the chatbot accurately responds to technical queries. The user-friendly interface is accessible on web and mobile platforms. Machine learning enhance accuracy over time, and data is updated regularly to stay current.

The chatbot undergoes actually beta testing with industry professionals for feedback and refinement before its official launch. Rheinfelden offers training and support materials to maximize usage. It's important to distinguish AI chatbot responses from human customer

support. The chatbot explains existing knowledge, while human support creates new solutions. Combining both utilizes AI's efficiency and human creativity.

One could say in a modified version of philosopher Hegel's dialectic ^[16]: Present your ideas (thesis) to AI, consider the AI's response (antithesis), and find together the best solution (synthesis). With this tool, you have a strong partner by your side.

2 Experiments

2.1 Primary aluminum

Low-carbon primary aluminum from Rusal provided the material for this research. The use of hydropower for electrolysis specifically reduced the Scope 3 carbon footprint to 3.5 tons of CO_{2-eq} , per ton of aluminum [6].

2.2 Secondary aluminum

Terms for secondary aluminum are not standardized and may vary. Therefore, the material used will be described here according to its type.

In this study, only post-consumer scrap was used, meaning scrap originating from end-users; for examples see the list below. Industrial scrap (pre-consumer recycling) was not considered. This point has a big impact on the calculated CO_{2-eq.} level.

The melt for all investigated alloys was cleaned using a gas treatment process with argon (Ar) and chlorine (Cl) to ensure effective impurity removal while maintaining economic efficiency. For the Magsimal alloys, an active gas treatment was applied to achieve enhanced melt quality.

The following scrap types were used:

- Wheels
- Profiles
- Litho
- Rod
- UBC

One of the highest-quality sources of secondary aluminum for AlSi cast alloys is wheel scrap. The low iron (Fe) content in wheels makes them particularly suitable for producing ductile AlSi alloys. To avoid the formation of brittle AlSiFe phases in AlSi alloys, it is essential to maintain a low Fe content. Because Fe is a highly stable element in aluminum and removing it requires significant energy, the simplest solution is to use scrap with inherently low Fe content.

Wheels typically contain 7% or 10% silicon (Si) and approximately 0.3% magnesium (Mg). The Mg content can be reduced through gas treatment of the molten metal.

In Europe, the high demand for wheel scrap has led to

limited availability and increased purchase prices.

Profiles from the 6000 series primarily contain magnesium (Mg) and silicon (Si). In the case of post-consumer recycling, various contaminants are expected due to mixing, especially the ubiquitous presence of iron (Fe). In contrast, industrial scrap (pre-consumer recycling) offers significantly higher quality.

Litho refers to printing plates used in lithographic printing. This material is characterized by low contamination, although it typically has a higher iron (Fe) content.

Rod is usually available as industrial scrap generated during wire production. In Europe, some overhead power lines are being replaced, making post-consumer rod available, though in limited quantities.

UBC stands for used beverage cans, which are widely available and have been recycled for many years through a well-established industry. While reusing old cans to produce new ones is common practice, it often results in a gradual decline in quality. Typically, a blend of old cans and primary aluminum is used to manufacture new ones. Typical elements in UBC are Mn up to 0.9 %, Fe, Si and Cu. Using this type of scrap for structural components is an excellent example of upcycling, as it converts high-volume, lower-quality scrap into valuable, high-performance products.

2.3 Investigated alloys

Several alloy families were tested in this study. Descriptions of the standard versions of these alloys are available on the Rheinfelden website, catalogues and publications [17-21].

The primary versions served as benchmarks and were compared to several secondary versions. The primary versions of Castasil-37, Silafont-36, and Castaduct-42 were produced with TiB₂ grain refinement, while all other alloy variants were produced without grain refinement.

Measurements were taken directly from the crucible immediately before the start of each casting series.

First focus was on AlSi-alloys, specifically Castasil-37 and Silafont-36, each with varying silicon content. The following variants were tested (see table 1):

- No. 1.1: Castasil-37, produced using 100% primary aluminum (benchmark).
- No. 1.2 to No. 1.4: Castasil-37 variants made using 50% wheel scrap.

Table 1. Castasil series (wt.%, Al bal.)

No.	Si Mn	Mg	Fe	Mo	Zr
-----	-------	----	----	----	----

1.1	9.56	0.49	0.01	0.13	0.13	0.13
1.2	5.23	0.45	0.07	0.20	0.13	0.13
1.3	7.80	0.44	0.08	0.20	0.12	0.13
1.4	10.00	0.45	0.05	0.22	0.12	0.13

(all alloys modified with appr. 100 ppm Sr)

Table 2 shows Silafont-36, Silafont-33, and Castaman-35 alloys, with the following versions tested:

- No. 2.1: Silafont-36, produced using 100% primary aluminum (benchmark).
- No. 2.2: Corresponding to the Silafont-33 alloy, made with 50% wheel scrap.
- No. 2.3 and No. 2.4: Corresponding to the Castaman-35 alloy, both versions made with 50% wheel scrap.

Table 2. Silafont series (wt.%, Al bal.)

No.	Si	Mn	Mg	Fe	Cu	Zn
2.1	10.33	0.61	0.33	0.11	0.00	0.00
2.2	7.03	0.48	0.36	0.18	0.02	0.02
2.3	8.60	0.49	0.35	0.16	0.01	0.01
2.4	10.02	0.49	0.36	0.18	0.02	0.02

(all alloys modified with appr. 100 ppm Sr)

The Castaduct alloy family was also tested, focusing on various compositions and scrap content:

- No. 3.1: Castaduct-42, produced using 100% primary aluminum (benchmark).
- No. 3.2: Castaduct-42 variant made with 25% rod and litho scrap.
- No. 3.3: Castaduct-42 Eco, produced with 50% profiles from the 6000 series.
- No. 3.4: Castaduct-51, made with 90% used beverage cans (UBC).

Table 3. Castaduct series (wt.%, Al bal.)

No.	Si	Mn	Mg	Fe	Cu	Ca
3.1	0.04	0.01	3.77	1.19	0.00	0.08
3.2	0.10	0.03	3.75	1.16	0.00	0.08
3.3	0.26	0.03	3.81	1.07	0.03	0.10
3.4	0.37	0.79	4.20	1.17	0.18	0.09

The AlMg6Si2Mn alloy family was also evaluated with different compositions:

- No. 4.1: Magsimal-plus, produced using 100% primary aluminum (benchmark).
- No. 4.2: Magsimal-plus variant made with 25% wheel scrap.
- No. 4.3: Corresponding to Peraluman-86 alloy, made of 90% sheet from the 6000 series.

Table 4. AIMg6Si2Mn series (wt.%, Al bal.)

		9 -		(,	,		
No.	Si	Mn	Mg	Fe	Cu	Zn	

4.1	2.09	0.51	6.19	0.14	0.00	0.00
4.2	2.34	0.53	6.01	0.15	0.00	0.00
4.3	2.34	0.45	6.11	0.38	0.22	0.29

No. 4.1 and No. 4.2 included additions of 30 ppm beryllium (Be), while No. 4.3 contained 0.1% calcium (Ca) and all 3 alloys 0.025 vanadium (V) to minimize melt oxidation.

2.4 Experimental setup

The Tech Center Rheinfelden is equipped with state-of-the-art machinery to support advanced aluminum alloy development and high-pressure die-casting (HP-DC) processes, see figure 2.

It features an electric melting furnace manufactured by Striko Westofen, a crucible with a capacity of 300 kg. The furnace is designed for efficient melting operations, ensuring precise temperature control and energy efficiency.

For gas treatment, the center uses a system developed by Fuco Heg, customized to Rheinfelden's specifications. This system allows for effective treatment of molten aluminum using argon and chloride gases, ensuring high metal purity and quality.

Alloy composition is carried out manually, utilizing a mix of primary aluminum, scrap, and master alloys to achieve specific material properties. The facility includes a 400-ton high-pressure die-casting cell equipped with a Fondarex vacuum system to enhance casting quality by reducing porosity. Dosing is performed manually with a ladle. During the die-casting process, manual spray application was performed using Chem-Trend SL-68012, diluted at a ratio of 1:100 in water.



Fig. 2: High pressure die casting cell in the Tech Center Rheinfelden

The test samples produced were $250 \times 60 \times 3$ mm plates, as shown in Figure 3. The ingate system used was a classic fan design featuring a 60×1.5 mm ingate to ensure even metal flow into the mold cavity. Additionally, the design included 4 overflows attached to the side to manage excess metal and improve the filling process. A venting system with chill vents is incorporated to facilitate proper venting and reduce gas entrapment.



Fig. 3: Shot of sample plate

3 Results and discussion

3.1 Mechanical properties

The following tables present the results of tensile testing, with most data collected in status F (as cast), except for the Silafont series. Each value represents the average of at least six samples, ensuring reliable and consistent data.

The bending angle (BA) is also reported, which serves as an indicator of rivetability. A bending angle of 60° is considered excellent, indicating ease of riveting, while a value of 30° is regarded as poor. However, a lower bending angle does not necessarily preclude riveting; it may deteriorate the joining quality or require additional measures on the process.

Table 5. Castasil series, status F

rubio di Guotadii dollodi, diatad i				
No.	US	YS	A	BA
	[N/mm ²]	[N/mm ²]	[%]	[°]
1.1	263	119	10.6	40
1.2	216	90	14.9	47
1.3	248	107	10.6	38
1.4	266	118	7.2	32

As the silicon content increased, strength improved while ductility decreased. When comparing 100% primary aluminum with 50% secondary aluminum at the same silicon level (samples 1.1 and 1.4), lower ductility was observed.

The results of the Silafont series in various heat treatment conditions are presented in Table 6, with the parameters for T5 and T6 treatments also specified. After T5 heat treatment, there was a simple colling in still air. In the T7 heat treatment, "air" refers to quenching by an air blower, a method commonly used in industrial production for structural components.

Table 6. Silafont series

No.	US	YS	A	BA	
	[N/mm ²]	$[N/mm^2]$	[%]	[°]	
	S	tatus F (as ca	ast)		
2.1	276	127	8.1	35	
2.2	248	119	7.5	30	
2.3	260	129	6.5	28	
2.4	274	138	5.3	26	
	Status T5 (200 °C 2 h)				
2.1	303	208	4.5	19	
2.2	284	196	5.3	20	
2.3	303	214	4.5	21	
2.4	312	215	4.6	20	
Statu	s T7 (465 °C	240 min. / ai	ir / 225 °C 80	min.)	
2.1	212	131	14.4	61	
2.2	201	137	12.5	61	
2.3	194	128	14.6	60	
2.4	210	141	11.1	57	

Similar to the results of the Castasil series, a high silicon content led to increased strength but reduced ductility. The difference in ductility between the F, T5, and T7 conditions was significant. While the difference in mechanical properties between 100% primary aluminum and 50% secondary aluminum (2.1 and 2.4) is clearly noticeable, it remains considerably smaller than the variations caused by different heat treatments.

Table 7. Castaduct series, status F

No.	US	YS	A	BA
	[N/mm ²]	[N/mm ²]	[%]	[°]
3.1	244	110	17.4	61
3.2	240	111	17.0	61
3.3	246	120	15.5	53
3.4	278	152	10.2	40

Table 7 shows the results of the Castaduct series. Remarkable was the high ductility, achieved in status F. No. 3.4 showed still an elongation and a bending angle that is equal to 1.1 and 2.1, in spite of the use of 90 % UBC scrap.

A bending angle of 60° was only achieved by 2.1-2.3 after T7 heat treatment.

Table 8. AlMg6Si2Mn series, status F

No.	US	YS	A	BA
	[N/mm ²]	$[N/mm^2]$	[%]	[°]
4.1	348	206	10.0	42



4.2	321	190	10.8	38	
4.3	298	208	3.4	14	

The AlMg6Si2Mn series (shown in table 8) stands out for its high strength. The use of 25% wheel scrap (4.2) was feasible without significantly affecting the mechanical properties. However, the use of 90% profile scrap (4.3) resulted in poor ductility.

3.2 Carbon footprint calculation

The certified carbon footprint calculation in Rheinfelden accounts for emissions related to materials and production processes up to the factory gate (cradle-to-gate). The use of low-carbon primary aluminum results in 4.61 tons of CO_{2-eq.} per ton of aluminum, a figure achieved using hydroelectric power during the electrolysis process.

Here are some values for the alloying elements. For silicon, the carbon footprint is 7.28 tons of CO_{2-eq.} per ton of silicon, while magnesium contributes 28.81 tons of CO_{2-eq.} per ton of material. The carbon footprint for manganese is 5.48 tons of CO_{2-eq.} per ton of manganese. Most values for alloying elements are given by the German Federal Office for Export and Economic Control that must be used in Germany if no certification about the carbon footprint is delivered by the supplier of the element (which is usually the case) [14].

In comparison, secondary aluminum, such as AlSi7Mg derived from wheel scrap, results in a significantly lower carbon footprint of 0.14 tons of CO_{2-eq.} per ton of aluminum, which includes emissions from accompanying elements like silicon. Transport emissions from Rheinfelden to the customer are not taken into account for the results shown in table 9. This method ensures an accurate carbon footprint assessment and supports sustainable practices in aluminum production.

Table 9. Carbon footprint

No.	ton CO ₂ -eq.	No.	ton CO ₂ -eq.
	per ton alloy		per ton alloy
1.1	5.66	2.1	5.64
1.2	3.16	2.2	3.26
1.3	3.30	2.3	3.34
1.4	3.44	2.4	3.44
3.1	5.92	4.1	7.22
3.2	4.66	4.2	6.05
3.3	3.51	4.3	3.02
3.4	1.68		

3.3 Castability

Castability in high-pressure die casting is challenging to

quantify accurately, which is extensively described in literature [22, 23]. In many cases, die casting defects dominate the properties of the component [24]. In high-pressure die casting, castability can be described as geometric constraints for the casting within which the occurrence of casting defects does not exceed an acceptable level. One of these limitations is the flow length and thus size of a casting, but also the local thickness, flow deflections, filling time, dynamic impact at the end of the filling phase and much more. There is no universally accepted value that would define castability in high-pressure die casting.

The results obtained from casting spirals using gravity casting often do not correlate well with high-pressure die casting processes. Various casting trials utilizing meander dies of different sizes provide useful indications but cannot deliver precise measurements.

One frequently considered criterion for assessing castability is the heat of fusion. The measurement is challenging, not all institutes provide consistent parameters [25-27]. The heat of fusion for several alloys was measured by the Light Materials and Technologies Institute (LMIT, UC RUSAL), as shown in Table 10. The values for 1.1, 2.1 and 2.2 were calculated by phase simulation taking into account measurement data of the LMIT.

Table 10. Heat of Fusion

No.	Alloy	kJ/kg
1.1	Castasil-37	471
2.1	Silafont-36	474
2.2	Silafont-33	450
3.1	Castaduct-42	367
4.1	Magsimal-plus	389

A high heat of fusion generally indicates good castability, particularly for small components. However, for larger castings, a high heat of fusion may not always be advantageous. It can lead to increased die wear, prolonged solidification times, and a greater reliance on a well-developed die temperature control system. Additionally, a significant amount of energy is required to melt alloys with a high heat of fusion, resulting in a less efficient production process. Nonetheless, the debate regarding the necessity of a high heat of fusion for large castings remains ongoing.

Silicon is generally a dominant element in aluminum alloys due to its high heat of fusion [28]. The results of the study are strongly influenced by the silicon content. In the case of AlSi alloys (1.1, 2.1, 2.2), silicon positively affects shrinkage, improving casting performance. At

first glance, this might suggest that silicon content is the sole decisive factor for castability. However, other factors also play a significant role in determining the overall castability of the alloy.

The chemical attack of aluminum alloys on die steel is another critical factor influencing castability. To assess this, the Austrian Foundry Institute (OGI) conducted tests to measure the erosion of hot-work die steel samples (1.2343, X38CrMoV5-1). These steel samples were rotated in an aluminum melt, and their weight loss was recorded over time. A more detailed description of the test device can be found in [19].

Table 11. Erosion results

No.	Alloy	Weight loss [%] after			
		2 h	4 h	8 h	16 h
1.1	Ci-37	12	17	32	52
2.1	Sf-36	7	16	30	45
3.1	Cc-42	2	6	12	14
4.1	Ma-plus	7	9	13	20

Table 11 presents the results for the weight loss of the die steel samples, expressed as a percentage. As anticipated, the low-iron alloys Castasil (1.1) and Silafont (2.1) exhibited similar erosion levels. In comparison, Magsimal-plus (4.1) performed significantly better, while Castaduct-42 (3.1) demonstrated the lowest level of chemical attack against die steel.

3.4 Welding

The alloys Castasil and Silafont (1.1 and 2.1) have been used in series applications for welding for many years. Numerous publications document the use of MIG, laser, friction stir, and other welding techniques for these alloys [29-35]. Among these, MIG welding remains the most commonly employed method for structural components due to its reliability and efficiency.

The alloys Castaduct and Magsimal (3.1 and 4.1) were successfully MIG welded without significant issues. The weld seams exhibited good geometry and low porosity, as shown in figures 4 and 6. Selecting the appropriate wire for each alloy series was essential, as indicated in table 12.

Table 12. Used welding consumables

		•
No.	Alloy	Consumable
1.1	Castasil	AlSi12
2.1	Silafont	AlSi12
3.1	Castaduct	AlMg4.5Mn
4.1	Magsimal	AlMg4.5Mn

Due to the rapid solidification during the welding process, the resulting microstructures were very fine, similar to the fine structure seen in high-pressure die castings, as depicted in figures 4 and 6.



Fig. 4: MIG-weld seam No. 3.1 (Castaduct-42)

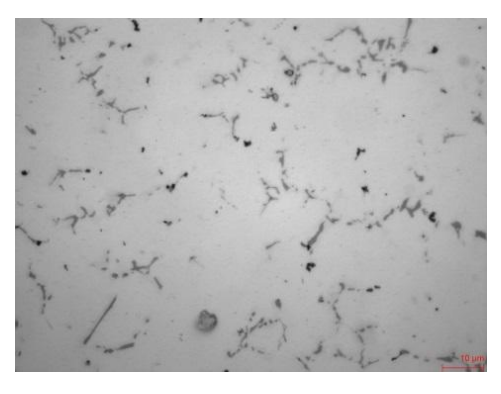


Fig. 5: Micrograph MIG weld seam No. 3.1, magnitude 1000 times



Fig. 6: MIG-weld seam No. 4.1 (Magsimal-plus)

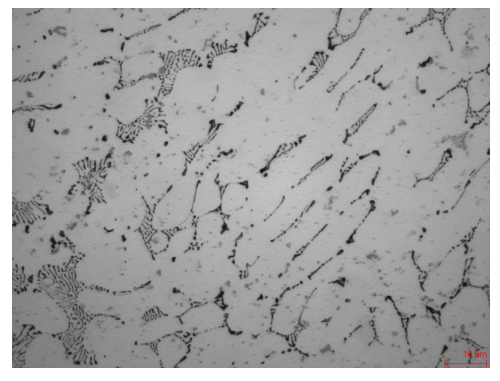


Fig. 7: Micrograph MIG weld seam No. 4.1, magnitude 1000 times

3.5 Salt spray tests

The corrosion resistance was evaluated using two classic

salt spray tests. The specimens consisted of 3 mm test plates cast in the Tech Center of Rheinfelden. The tests were conducted over a duration of 720 hours at ambient temperature, using a spray medium of 5% NaCl in water.

The first test was assessed by measuring the maximum depth of corrosion attack observed in a micrograph (carried out by STZ Friedrichshafen, Germany). The results are presented in Table 13.

Table 13. First salt spray test

No.	Alloy	Max. depth of corrosion
		attack [µm]
1.1	Castasil-37	150
3.1	Castaduct-42	15
4.2	Magsimal-plus	30

The results of the first test reveal significantly lower corrosion attack for 3.1 (Castaduct-42) and 4.2 (Magsimal-plus) compared to 1.1 (Castasil-37). It is noteworthy that the corrosion resistance of Castasil-37 has been successfully utilized in series applications for over two decades.

The second test evaluated the weight loss of the plates (carried out by the Light Materials and Technologies Institute UC RUSAL). The results are presented in Table 14.

Table 14. Second salt spray test

No.	Alloy	Weight loss	
		[g/(m² day)]	
2.1	Silafont-36 F	0.12	
2.1	Silafont-36 T6	0.09	
3.1	Castaduct-42	0.09	
3.2	Castaduct-42	0.11	
3.3	Castaduct-42 eco	0.19	
3.4	Castaduct-51	0.30	

The results of the second test indicate a comparable level of corrosion resistance between Silafont-36 and Castaduct-42. As anticipated for AlSi alloys, the corrosion resistance improved with the application of a T6 heat treatment. However, an increased proportion of secondary material, and consequently a higher concentration of impurities, resulted in reduced corrosion resistance, as observed in examples 3.3 and 3.4.

Additional salt spray tests revealed that incorporating 0.2% copper into Silafont-36 significantly increased the weight loss to 1.0 g/(m²·day) in the as-cast condition. However, applying a T6 heat treatment notably enhanced the alloy's corrosion resistance.

3.6 Electrical Conductivity

The following tables present the electrical conductivity of Castasil, Silafont, Castaduct, and AlMg6Si2Mn alloy series, measured at room temperature ($20 \pm 0.5^{\circ}$ C). Electrical conductivity values are reported in [MS/m -%IACS], and the standard deviation between measurements is consistently less than 0.3, indicating high precision values.

Table 15: Castasil series

No.	Electrical Conductivity
	[MS/m - %IACS]
1.1	-
1.2	18.78 - 32.39
1.3	17.81 - 30.70
1.4	16.59 - 28.60

The table 15 shows the electrical conductivity of the Castasil series in the as-cast condition (F). The measured values range from 16.59 MS/m to 18.78 MS/m, indicating relatively consistent conductivity among the samples in this series.

Table 16 includes electrical conductivity measurements for the Silafont series in the as-cast condition ("F"), and T5 (200°C for 2 hours) and then T7 (465°C for 40 min. /air/225°C 80min.) heat treatments.

The electrical conductivity of Silafont alloys improves significantly from the as-cast (F) condition to T5 and T7 heat-treated states due to microstructural changes. The heat treatments improve conductivity by cleaning up the aluminum matrix and refining the microstructure making Silafont a prime example of how heat treatments can enhance the properties of an alloy.

Table 16: Silafont Series

No.	Electrical Conductivity		
	[MS/m - %IACS]		
	Status F (as cast)		
2.2	17.66 - 30.45		
2.3	18.74 - 32.31		
2.4	17.61 - 30.36		
	Status T5 (200 °C 2 h)		
2.2	19.61 - 30.81		
2.3	21.32 - 36.76		
2.4	21.37 - 30.84		
Status T7 (465 °C 40 min. / air / 225 °C 80min.)			
2.2	23.33 -40.22		
2.3	24.14 - 41.62		
2.4	23.02 - 39.69		

Table 17 present values of Castaduct series a wide range of electrical conductivity from 12.94 MS/m to 18.52 MS/m at as cast "F" condition.

Table 17: Castaduct Series

No.	Electrical Conductivity
	[MS/m - %IACS]
3.1	18.39 - 31.70
3.2	18.52 - 31.93
3.3	14.39 - 24.81
3.4	12.94 - 22.31

Table 18 (AlMg6Si2Mn Series) lists electrical conductivity for the AlMg6Si2Mn series in the as-cast state, indicating relatively consistent conductivity between the samples in this series.

Table 18: AlMq6Si2Mn Series

No.	Electrical Conductivity
	[MS/m - %IACS]
4.2	13.51 - 23.29
4.3	13.29 - 22.91

4 Conclusions

The objective of the investigations was to evaluate the main characteristics of various alloy types for the production of large structural components.

This study reaffirmed that AlSi alloys are defined by their exceptional castability, which is attributed to their high heat of fusion and low shrinkage. They also possess favorable material properties, particularly after T6/T7 heat treatment, excellent weldability, along with good corrosion resistance when impurity levels are controlled.

Despite these advantages, Silafont alloys (2.1–2.4) exhibit certain limitations. Their moderate ductility in the as-cast condition restricts crash performance and rivetability, with a particularly low bending angle in both status F and T5 highlighting this shortcoming. Additionally, these alloys have a low tolerance for impurities – investigated with a maximum Fe content of 0.2% – which necessitates high-quality secondary aluminum. Furthermore, AlSi alloys are prone to corrosion in the as-cast state, as detailed in Chapter 3.5.

Castasil-37 (1.1) represents an advanced development of Silafont-36, designed to optimize mechanical properties in the as-cast state while reducing die wear, even with a low Fe content.

Reducing the silicon content from 10% to 7% enhances mechanical properties for defect-free castings. However, this reduction negatively impacts castability due to a lower heat of fusion and increased shrinkage, which raises the risk of die casting defects.

The ideal silicon content in AlSi alloys remains a topic of active investigations and debates. A potential optimal range may lie between 8% and 9%, balancing mechanical properties with castability.

The Castaduct alloy series (3.1–3.4) are a recently developed alternative to traditional AlSi alloys, offering significant advantages in specific applications. It demonstrates high ductility in the as-cast state, making it particularly suitable for applications requiring good crash performance and rivetability. The weldability was proven.

The alloy's high iron content contributes to reduced soldering and allows for shorter spray times during production. Additionally, its relatively low heat of fusion minimizes the need for extensive die temperature control, reduces solidification time, and results in significantly higher productivity due to shorter cycle times. Energy savings during melting are another advantage.

The composition of Castaduct alloys accommodates high levels of impurities, such as iron and other elements, without significantly compromising mechanical properties or corrosion resistance. These qualities make it an attractive option for structural components.

Currently undergoing qualification for structural applications, the alloy is slated for its first series applications starting in 2025.

The Magsimal alloy series (4.1–4.3) are specifically designed as a high-strength solution for structural components. Magsimal-plus, a further evolution of the well-established Magsimal-59 alloy, builds on decades of application in the industry.

Its primary advantage lies in its exceptional strength, which offers significant potential for lightweight construction, making it ideal for modern design requirements. Additionally, Magsimal alloys exhibit a high level of corrosion resistance, further enhancing their suitability for demanding structural applications where durability and reliability are essential.

The measurement of electrical conductivity provides a quantitative assessment of the extent of contamination. This approach enables the identification of contamination levels.

4.1 Outlook

AlSi alloys are expected to remain the standard for cast components. The objective of producing structural components without the need for heat treatment supports the continued application of Castasil-type alloys. Meanwhile, Castaduct and Magsimal alloys are likely to find niche applications. Their primary appeal lies in their mechanical properties in the as-cast state – particularly

the high strength offered by Magsimal-plus – and their ability to utilize scrap types that differ from those used for Silafont or Castasil alloys.

To enhance sustainability, the use of secondary aluminum and the practice of upcycling are crucial. Incorporating a high proportion of secondary aluminum has the most significant impact on reducing the carbon footprint of an alloy. It is vital to repurpose secondary aluminum with high levels of impurities; otherwise, these scrap types risk being relegated to downcycling. However, technical methods for removing impurities such as iron (Fe) or copper (Cu) from an alloy are limited.

Maximizing the value of each scrap type by using it in the highest-quality alloy possible is a critical principle in the aluminum recycling industry. Die casting, in particular, offers an advantage by allowing the re-use of lower-quality scrap compared to its application in sheet metal and extrusions.

The strength of an alloy has a dual impact on the carbon footprint of a cast component. Firstly, higher strength enables further lightweight construction, contributing to lower energy consumption during a vehicle's use phase. Secondly, reduced component weight translates to a decreased need for aluminum per component, significantly reducing the carbon footprint associated with its production. These combined benefits are expected to drive the increasing adoption of high-strength alloys in the future.

It can be expected that the development of standard alloys with higher secondary aluminum content will continue. The production of such standardized alloys in large volumes offers significant economic advantages. At the same time, the development of specialized alloys for niche applications will remain essential, driven by the constant need for innovation. The development of new alloys for very large castings is an active area of research and will persist until a new standard is established.

Acknowledgments

This paper was written with the help of ChatGPT and the Rheinfelden Chabot.

Thanks to the Light Materials and Technologies Institute (LMTI) of Rusal for their support.

Conflicts of interest

The authors declare that they have no known competing financial interests or personal relationships that could have appeared to influence the work reported in this paper.

References

- [1] Aluminum Stewardship Initiative (ASI). https://aluminium-stewardship.org. Accessed 09 Jan 2025.
- [2] TüvSüd. Carbon footprint verification and validation. https://www.tuvsud.com/de-de/branchen/energie/erneuerb are-energien/energiezertifizierung/carbon-footprint-verifiz ierung. Accessed 09 Jan 2025.
- [3] Schlesinger M E. Aluminum Recycling. ISBN-13: 978-1-4665-7024-5. CRC Press, Taylor and Francis Group, 2014.
- [4] Krone K. Aluminium-Recycling. ISBN 3-00-003839-6. Vereinigung Deutscher Schmelzhütten e.V. Düsseldorf, 2000.
- [5] International Aluminium Institute. https://aluminiumstewardship.org. Accessed 09 Jan 2025.
- [6] EN+ Group. Sustainability downloads. https://enplus group.com/en/sustainability/downloads. Accessed 09 Jan 2025.
- [7] Weiqiao. Environmental, Social and Governance Report. http://www.wqfz.com/public/upload/files/20220530/1653 906028.pdf. Accessed 09 Jan 2025.
- [8] Lizhong Group. Environmental, social and governace report. https://file.finance.qq.com/finance/hs/pdf/2023/04/25/121 6556763.PDF. Accessed 09 Jan 2025.
- [9] China Hongqiao. Sustainability. http://en.hongqiaochina. com/our_commitment.html#commitment2. Accessed 09 Jan 2025.
- [10] Chinalco. Performance Report. https://www.chalco.com. cn/en/tzzgxen/yjbgen. Accessed 09 Jan 2025.
- [11] Rio Tinto. Sustainability. https://www.riotinto.com/ sustainability. Accessed 09 Jan 2025.
- [12] Alcoa. 2023 Sustainability Report. https://www.alcoa. com/sustainability/en. Accessed 09 Jan 2025.
- [13] Hydro. Sustainabilty reporting. https://www.hydro.com/ en/sustainability/sustainability-reporting. Accessed 09 Jan 2025.
- [14] N. N. Informationsblatt CO₂-Faktoren. Volume 1.1, German Federal Office for Economic Affaires and Export Control (BAFA). Nov. 11, 2021.
- [15] German Federal Environment Agency. Probas datasheet. https://www.probas.umweltbundesamt.de/php/index.php. Accessed 09 Jan 2025.
- [16] Hegel G W F. Encyclopedia of the Philosophical Sciences in Outline. Heidelberg, Germany, 1817.
- [17] Rheinfelden. Families of Alloys. https://rheinfelden-alloys. eu/en/alloys/. Accessed 09 Jan 2025).
- [18] Rheinfelden. Leporello. https://rheinfelden- alloys.eu/wp-content/uploads/2018/08/Leporello-Aluminium-Casting-Alloys_RHEINFELDEN-ALLOYS_2018.pdf. Accessed

09 Jan 2025).

- [19] Wiesner S, Miller R. HP-DC Alloys for Structural Castings: AlMg4Fe2 and AlMg4Zn3Fe2 (Castaduct-42 and -18). NADCA Die Casting Congress and Tabletop, Indianapolis, Oct. 15-17, 2018
- [20] Wiesner S. Reduction of the Carbon Footprint of Al HP-DC Structural Components. NADCA Die Casting Congress and Tabletop, Grand Rapids, Sep. 19-21, 2023
- [21] Koch, H., Hielscher, U., Sternau, H. Silafont-36, the new low iron high-pressure die casting alloy. TMS light metals. NV/USA, 1995, p. 1011-1018).
- [22] [22] Ruhland, N. T. Druckgießen für Praktiker. ISBN 3-87260-136-9. Published by Gießerei-Verlag GmbH, Düsseldorf, 2003.
- [23] Hasse, S. Gießereilexikon. ISBN 978-3-7949-0753-3. 19th edition. Published by Schiele & Schön GmbH, Berlin, 2007.
- [24] Walkington, W. G. Die casting defects-causes and solutions. North American Die Casting Association (NADCA). Wheeling, USA, 1997.
- [25] Leitner M, Leitner T, Schmon A, Aziz K, Pottlacher G. Thermophysical Properties of Liquid Aluminum. Metallurgical and Materials Transactions A. Volume 48A, June 2017, p. 3036-3045. https://doi.org/10.1007/ s11661-017-4053-6
- [26] Mills K C. Recommended Values of Thermophysical Properties for Selected Commercial Alloys. Woodhead Publishing Ltd, Cambridge, United Kingdom, 2002, pp. 19 - 25.
- [27] Schmidt U, Vollmer O, Kohlhaas R. Zeitschrift für Naturforschung. Volume 25a, 1970, pp. 1258 – 64.
- [28] Jarfors E W, Jansson P. Selecting Cast Alloy Alloying Elements Suitable for a Circular Society. https://www.

- mdpi.com/2071-1050/14/11/6584. Accessed 09 Jan 2025.
- [29] Wiesner, S. Economic production of weldable aluminum high-pressure die casting. Doctoral thesis at the Technical University Brunswick, Germany. ISBN 3-8322-1388-0. Published by Shaker, Aachen, 2003.
- [30] Wiesner, S., Rethmeier, M., Wohlfahrt, H. MIG and Laser Beam Welding of Aluminium Die Castings with Wrought Aluminium Profiles. Joining Technologies of Dissimilar Materials and Structural Integrity Problems of so Joined Structures, IIW, Ljubljana, Slovenia, July 2001, p. 147-153.
- [31] Rethmeier, M., Wiesner, S., Pries, H.; Wohlfahrt, H. Metal inert gas (MIG), laser beam and laser hybrid welding of aluminium die castings for space frame constructions. Doc. 65, CIATF Technical Forum, Corea, 2002.
- [32] Rethmeier, M., Wiesner, S., Wohlfahrt, H. Weldability of Aluminium Die Castings. IIW Annual Report 2000 Commission IX, IIW Doc. IX-NF-07-00, IIW Doc. IX-1984-00, Geesthacht 21.-22.02.2000; Firenze 09.-14.07.2000.
- [33] Winkler, R. Porenbildung beim Laserstrahlschweißen von Aluminum- Druckguss. Doctoral thesis at the Technical University Stuttgart, Germany. ISBN 3-8316-0313-8. Published by Herbert Utz Verlag, München, 2004.
- [34] Katayama, S. Matsunawa, A., Kojiama, K., Kuroda, S. CO₂ laser weldability of aluminum alloys. Report 4, Effect of welding. Welding International, Volume 14, Issue 1, p. 12-18, 2000.
- [35] Katayama, S. Matsunawa, A., Kojiama, K. CO₂ laser weldability of aluminum alloys. Report 2, Defect formation. Welding International, Volume 12, Issue 10, p. 774-789, 1998.